REVISTA MATÉRIA V.25 N.04

ISSN 1517-7076 articles e-12883, 2020

Evaluation of nano-TiO_2 on properties of cementitious mortars

Cézar Augusto Casagrande [1], Lidiane Fernanda Jochem [2], Wellington Longuini Repette [3], Dachamir Hotza [4]

1 Technologic Center of Campus Agreste, Federal University of Pernambuco (UFPE), CEP: 55014-900, Caruaru, PE, Brazil.

2 Academic Department of Civil Construction (DACOC). Technological Federal University of Paraná (UTFPR), Curitiba, PR, Brazil.

3 Department of Civil Engineering (ECV). Federal University of Santa Catarina (UFSC), CEP: 88040-970, Florianópolis, SC, Brazil.

4 Department of Chemical Engineering (EQA). Federal University of Santa Catarina (UFSC), CEP: 88040-900, Florianópolis, SC, Brazil.

email: cezar.acasa@gmail.com; lidijochem@gmail.com; wellington.repette@gmail.com; dhotza@gmail.com

ABSTRACT

This work deals with the effect in fresh and hardened properties of nano-TiO_2 as addition in cement-based mortars. Three commercial nano-TiO_2 powders were characterized by laser granulometry, XRD, FRX, zeta potential, BET and SEM. Two cementitious mortars were produced with nano-TiO_2, an industrialized and a non-industrialized type; then, these mortars were characterized by flowability, surface roughness, flexural strength and surface fracture. The results showed that the nano-TiO_2 addition reduced the flowability in terms of spread on table of the mortars. For surface roughness, in the industrialized mortars, the nanoparticles resulted in a smoother surface, while in the non-industrialized mortars, the nanoparticles formed a rougher surface. For flexural strength, in the non-industrialized mortars, the higher the nanoparticles amount, the higher the strength, while in the industrialized mortars no tendency was verified. In addition, from SEM analysis, it was noted that the fracture of the samples presented a tortuous aspect and growth through the region between cement paste and aggregates.

Keywords: nano-TiO_2; cementitious mortar, flowability; flexural strength

1. INTRODUCTION

Cementitious mortars are one of the most used material for building engineering. They are applied in façade coating, floor and roof construction, brick settlement, ceramic tile fixing and others. For this, cementitious mortars are obtained from the homogeneous mixture of one or more binders (cement and lime), aggregate (< 4.8mm) and water, whether or not containing admixtures and mineral additions that may provide proper adhesion and hardening properties. Generally, cementitious mortar coating systems act on their functions and properties in conjunction with the substrate. The execution of cementitious mortar coatings requires particular mortar properties, such as plasticity to deform on the substrate surface upon release and application, flowability to surround substrate roughness and water retention to maintain workability during application.

For improving the mortar properties there are a huge amount of additives that may interfere in the fresh and hardened properties [1]. Normally, a polymeric addition has the objective to improve flowability and/or water retention, and the mineral addition seeks to enhance plasticity, porosity, adhesion and cost of the material, acting mainly in the fresh state.

For the hardened state, some techniques may be used; nevertheless, the mechanical strength is less relevant for some applications, as coating. In this case, low values of strength are required (in the order of 1 MPa for flexural strength [2], for example). In this way, a great quantity of mineral additives may be used as

Autor Responsável: Cézar Augusto Casagrande Data de envio: 10/10/2019 Data de aceite: 14/03/2020

10.1590/S1517-707620200004.1183

component to improve the mechanical properties or to reduce the binder consumption the cementitious composites.

Nanoparticles have been employed for improving many properties in cementitious materials [3–5], as flowability [6–8], increasing the spread of the cementitious pastes that may reflect in lower consumption of synthetic admixtures. Moreover, nanoparticles may enhance the cement hydration degree (i.e binder efficiency) through seeding effect due the high specific surface area that interacts with cement in hydration process [9,10], which may result in lower cement consumption or higher mechanical properties. In the same trend, the nanoparticles may act as nanofillers, improving the packing of the particles and the compactness of the matrix, which may improve durability due the lower total porosity of the final material [11]. Furthermore, another approach is the setting controlling by the incorporation of nanoparticles, which may retard or accelerate the cement hydration [12]. In addition, since mortars are mainly present in building façades, they may be used as substrates for active nanoparticles in their surfaces [13], as gas oxidants [14–16] and self-cleaner surfaces [17].

In this work, we propose the use of nano-TiO_2 as addition in cementitious mortars for coating materials. For this, two types of cementitious mortars were produced with three nano-TiO_2 types and nanoparticles concentration from 0 to 10% in relation to cement weight. In the fresh state, flowability in terms of spread on table was evaluated. For the hardened state, surface roughness was evaluated by indirect macrotexture measurement with fine sand; flexural strength by bending test; and fracture surface of the mortars by SEM.

2. EXPERIMENTAL

2.1 Materials

Three commercial titanium dioxide (TiO_2) nanopowders were used: P25 (Degussa, Germany), which corresponds to 80 wt% anatase and 20 wt% rutile; anatase (Crenox, Germany, named “C”); and anatase (Nanostructured Amorphous Materials Inc., USA, named “N”). The phase crystallinity characterization was made on a Miniflex-II Desktop X-Ray diffractometer (Rigaku), operating at 30 kV/15 mA, with Cu radiation, 1.5406 Å wavelength, scanning range of 20-80 degree of 2θ and scanning rate of 0.05 θ/s. The particle size distribution was evaluated on a Nano-Zetasizer model ZEN 3600 (Malvern) in a 1% aqueous dispersion. The BET specific surface area analysis was performed in a Nova 1200e (Quantachrome). The chemical composition was determined by XRF in a PW 2400 spectrometer (Phillips). For microstructural analysis, secondary electrons images were obtained in a XL30 SEM (Philips).

For Zeta potential analysis, a Nano-Zetasizer ZEN 3600 (Malvern) was used. For the characterization, 1% aqueous dispersion acidified with HCl 1M was used, and titration with NaOH 0.25M until pH 9.5 was performed. This analysis shows the electric charge in the system and the isoelectric point (IEP) as the region in the graph that corresponds to no electric charge in the particles surface, indicating the maximum agglomeration potential.

Two types of mortars were produced, an industrialized ready mixed and a non-industrialized mortar mixed in laboratory, for comparison. For the industrialized mortars, a ready mixed mortar (Votomassa, from Votorantim Cements), was used. The chemical composition of the cement CP-II F 32, used in this type of mortar is shown in

Table **1**. For the non-industrialized mortars, a CP-II Z 32 cement was used (

Table **1**) and a quartz sand with maximum diameter of 4.8 mm and 2.36 finesses modulus was used as aggregate. The particle size distribution of the sand is presented in Figure. 1.

The nano-TiO_2 was added in proportions of 3, 5, 7 and 10 wt% relative to cement, as given in Table 2.

Table 3 presents the materials proportion for production of the mortars. The samples were molded, then cured during 1 day at t 25 ±2 °C and RH of 60 ±5%. Then, the samples were cured at 25±2 °C and >99% relative humidity (RH) in a wet room during the next 6 days before being transferred to a controlled room at 25±2 °C and RH of 60±5%.

Table 1: Properties of Portland cements used.

COMPOUND	CEMENT (wt%)	
	CPII-F 32	CP II-Z 32
CaO	60.26	54.35
SiO_2	18.7	21.49
MgO	4.86	3.15
Al_2O_3	4.27	6.36
Fe_2O_3	2.73	3.18
SO_3	2.7	2.66
$K_2O + Na_2O$	0.72	0.84
Insoluble residue	1.09	10.88
Loss on Ignition	4.28	6.51

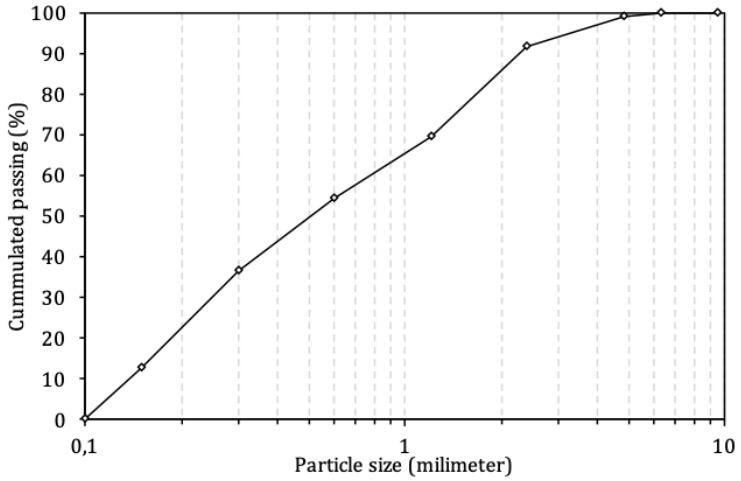

Figure. 1: Particle size distribution of the quartz sand.

Table 2: Composition of the mortars.

	SAMPLE	MATERIAL (weight proportion)				
		CEMENT	SAND (< 4.8 mm)	WATER	ADMIXTURE [a]	nano-TiO_2
Industrialized mortars	REF_I (0%)	1	4.879	0.84	0.0028	-
	I_3 %	1	4.879	0.84	0.0028	0.03
	I_5 %	1	4.879	0.84	0.0028	0.05
	I_7 %	1	4.879	0.84	0.0028	0.07
	I_10 %	1	4.879	0.84	0.0028	0.1
Non-industrialized mortars	REF_N (0%)	1	6.00	0.75	0.25	-
	N_3 %	1	6.00	0.75	0.25	0.03
	N_5 %	1	6.00	0.75	0.25	0.05
	N_7 %	1	6.00	0.75	0.25	0.07
	N_10 %	1	6.00	0.75	0.25	0.1

[a] For industrialized mortars, an air-entraining admixture was used. For non-industrialized mortars, a superplasticizer admixture was used. The superplasticizer was used due only the air-entraining was not efficient to promote a spread on table equivalent to the industrialized mortar.

Table 3: Constituent consumption for mortars.

Constituent ($kg \cdot m^{-3}$)	INDUSTRIALIZED MORTARS					NON-INDUSTRIALIZED MORTARS				
	REF_I	I_3%	I_5%	I_7%	I_10%	REF_N	N_3%	N_5%	N_7%	N_10%
Cement	330.4	329.6	329.1	328.5	327.7	278.6	278.0	277.6	277.3	276.7
Sand	1612.2	1608.3	1605.7	1603.1	1599.3	1671.8	1668.4	1666.1	1663.9	1660.5
Water	277.5	276.9	276.4	276.0	275.3	208.9	208.5	208.2	207.9	207.5
Admixture	0.9	0.9	0.9	0.9	0.9	69.6	69.5	69.4	69.3	69.1
Nano-TiO_2	0.0	9.8	16.4	23.0	32.7	0.0	8.3	13.8	19.4	27.6
$\sum$	2221.1	2225.6	2228.6	2231.6	2236.1	2229.1	2232.9	2235.4	2237.9	2241.7

Note: The consumption of materials was calculated considering the respective specific gravity values: cement 3.11 $g \cdot cm^{-3}$ for CP II F and 2.97 $g \cdot cm^{-3}$ for CP II Z, sand 2.62 $g \cdot cm^{-3}$, water 1.00 $g \cdot cm^{-3}$, admixture 1.10 $g \cdot cm^{-3}$ and nano-TiO_2 4.10 $g \cdot cm^{-3}$.

2.2 Methods

2.2.1 Fresh and hardened properties

The mixing of the mortars were carried out in a planetary rotation mechanical mixer for 5 min. The fresh state properties of the cement mortars were evaluated by workability in terms of spread on table, based on the standard ABNT NBR 13276 [18]. The mechanical properties of the cement mortars were assessed by three point bending tests adapted from the standard ABNT NBR 13279 [19]. Three samples of each series were measured at 28 days of cement hydration. The samples dimensions were 20 × 40 × 120 (height × width × length) in mm, and the span between the lower supports was 80 mm.

A surface macrotexture analysis was performed according to an adapted test from ASTM E-965 [20]. The objective was to verify the roughness of the surface of the mortar using 200 × 400 mm samples [15]. The test consists in spreading sand, passing through 0.25mm sieve, on the surface of the mortar sample through circular motions with a standardized socket. The diameter of the spot is measured in four orthogonal directions. In addition, after mechanical tests, the mortar surfaces were analyzed by SEM.

3. RESULTS AND DISCUSSION

In Figure 2, XRD patterns of the nano-TiO_2 powders used in this work are presented. P25 is commercialized as a mix of anatase and rutile phases; both crystal phases were identified in the samples. The other powders C and N are commercialized as anatase phase. It was possible to note that the main characteristic peak of rutile phase in ~31° is identified only in P25. The other peaks, as in ~66° and ~72° detected in C and N powders are due to rutile residues from production process. For photocatalysis, a mix proportion of anatase and rutile is normally used [21], such as in the case of P25 [14, 22, 23]. Cementitious materials with nano-TiO_2 are cited using anatase/rutile mix [13], rutile [24] and anatase phase [25]. However, in those cases, the main goal is the photocatalytic behavior, and the effect of the type of TiO_2 phase on the matrix properties was usually not exploited.

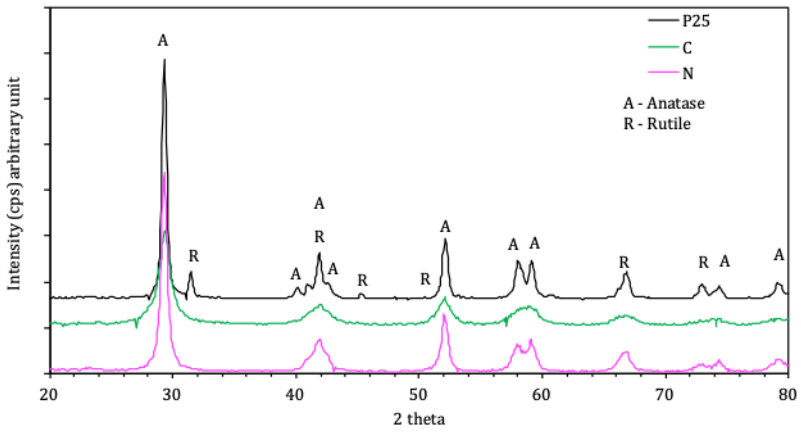

Figure 2: XRD patterns compared to ICSD patterns of anatase [26] and rutile [27], 172914 and 167953 codes, respectively.

Figure 3 shows the particle size distribution (PSD) of the nano-TiO_2 powders used in this work. It is possible to note that P25 is the finest material, followed by N, and C. In addition, P25 presented a more graduated distribution, in comparison with N and C samples. The D_{50} are 314, 660 and 876 nm for P25, N and C, respectively. For these particles configuration, the narrow distribution presents the higher potential to contribute in the binder hydration kinetics. In the so called "seeding effect", ionized surfaces lead the main product of the cement hydration (calcium silicate hydrated, C-S-H) to precipitate. In this case, the coarser the distribution of the nanoparticles, the higher is the potential for the filler effect, which corresponds to the better particle packing that also may enhance the hardened state properties of the cementitious matrix.

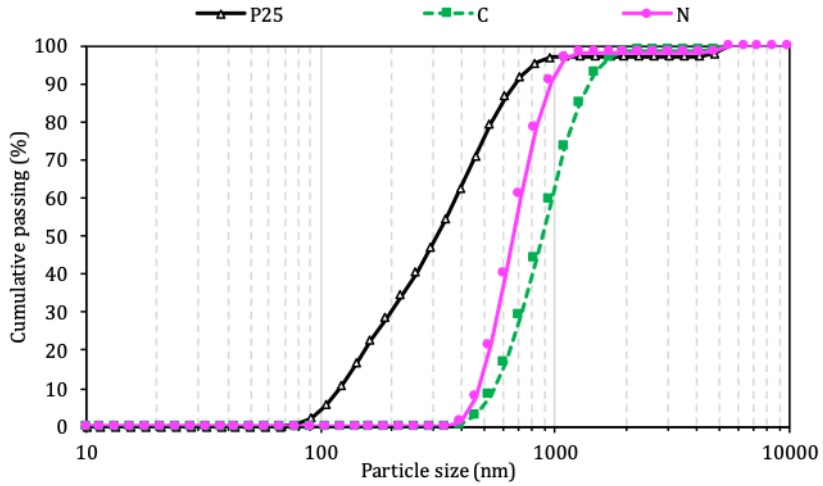

Figure 3: PSD of the nano-TiO_2 powders used.

Figure 4 presents the microstructures of the nano-TiO_2 powders with magnification of 15000× and a zoom of 70000×. In Figure 4 (a), the P25 powder particles are smaller than 100 nm; however, the particles are agglomerated due the high specific surface area available. According to the PSD, the particles present values higher than 100 nm, which confirms the agglomeration. For nano-TiO_2 C and N powders, Figure 4 (b) and (c), respectively, the agglomeration is even more evident. It is possible to verify the groups of nanoparticles that are close to 500 nm (as verified in PSD); nevertheless, in the zoom, it is possible to note that the particles present less than 100 nm, indicating a high tendency to agglomeration. This is expected once as lower the particle size, due the higher the surface energy.

These characteristics of the nanoparticles may present two effects on the mortar: either to reduce potential effect in the paste reaction (reflected in higher spread value, for example) or to accelerate the cement reactions by the nanoparticles presence in the cementitious paste. In this case, the average particle size is 500 nm, which might give an additional surface area for chemical ionization.

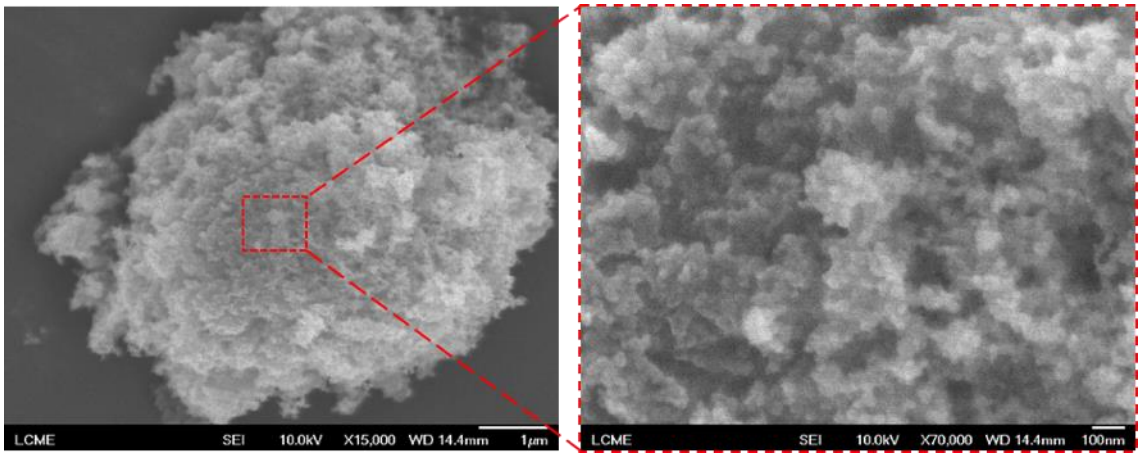

(a)

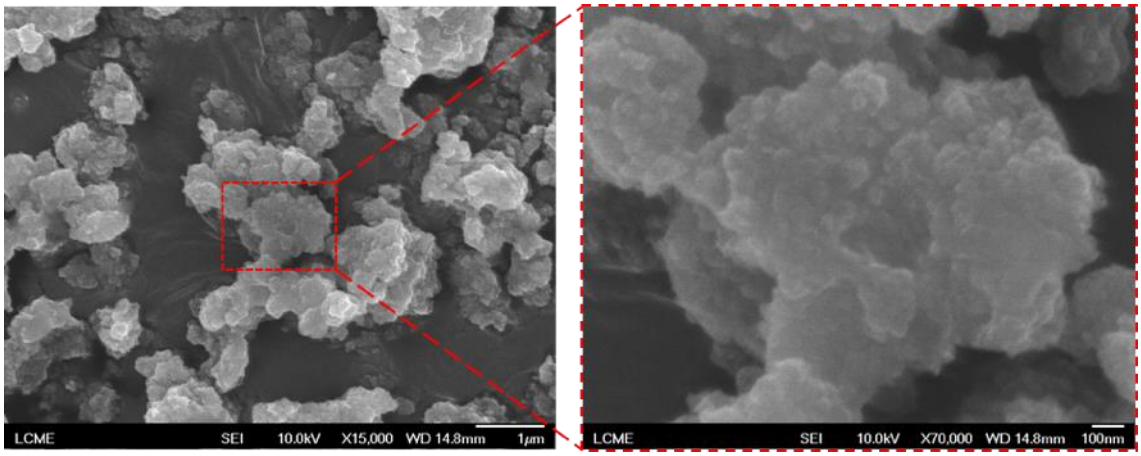

(b)

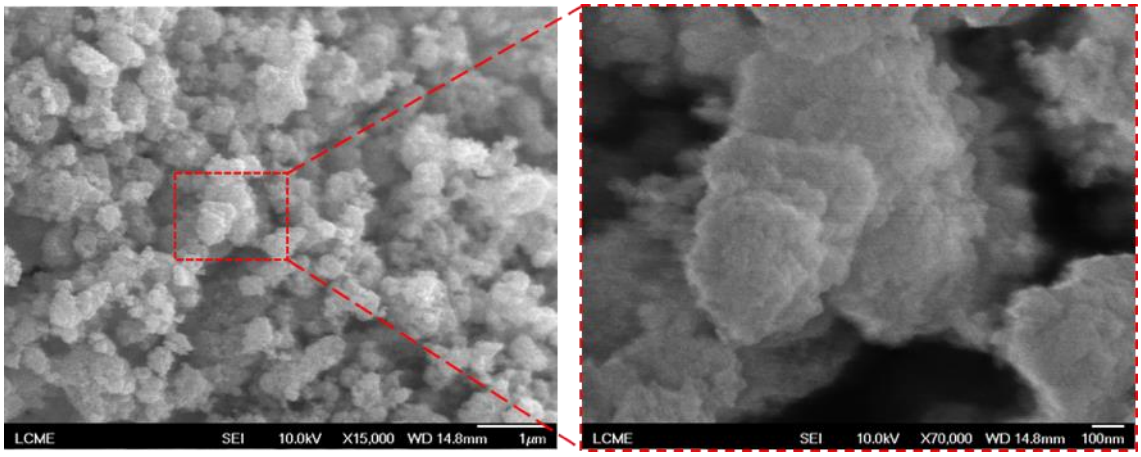

(c)

Figure 4: Microstructures (SEM) of the nano-TiO_2 powders. (a) P25; (b) C; (c) N.

Table 4 presents the chemical properties of the nano-TiO_2 powders used in this work. The P25 and N nano-TiO_2 powders present more than 96% TiO_2, and less than 0.17% of all others oxides detected, which demonstrates the high purity of the materials. The C nanopowder has >78% TiO_2 and ~7% of loss of ignition,

which corresponds to carbonaceous particles in the composition. Additionally, probably due to the production process by chlorination, it also presents >10% SiO_2, which is related to silica addition to reduce the cost of the final product.

Table 4: Chemical properties of the nano-TiO_2 powders.

COMPOUND	Nanopowders (wt%)		
	P25	**C**	**N**
TiO_2	97.83	78.37	96.2
CaO	<0.05	0.06	0.09
SiO_2	<0.05	10.7	<0.05
MgO	0.10	0.09	0.12
Al_2O_3	<0.05	<0.05	<0.05
Fe_2O_3	<0.05	<0.05	<0.05
P_2O_5	<0.05	0.48	0.17
K_2O	<0.05	<0.05	<0.05
Na_2O	0.09	3.15	0.09
BaO	0.09	0.09	0.08
MnO	<0.05	<0.05	<0.05
Loss on Ignition	1.81	7.06	3.21

In Figure 5, it is presented the zeta potential (ZP) of the nano-TiO_2 powders used in this work. It is possible to note that P25 shows the highest ZP among the powders. From pH 3 to 9.5, ZP is between 20mV and -20mV that is an interval that may lead to particle agglomeration. The PIE was detected at pH 7.23, and a tendency to maintain this value for higher pH corresponds to the agglomeration detected by PSD and microstructural analysis (Figure 3 and Figure 4, respectively). This also indicates an agglomeration potential in natural environmental of cementitious matrix, that is pH 12.5. For N and C powders, ZP begins with values lower than 20 mV and decreases as the pH value increases. However, after pH 6, ZP is lower than -20mV, and continues decreasing for higher pH values, indicating a high dispersion potential in the natural environment of cementitious matrix. The PIE of N and C nanopowders were in pH 5.20 and 3.91, respectively, indicating a great potential for dispersion in cementitious mixtures.

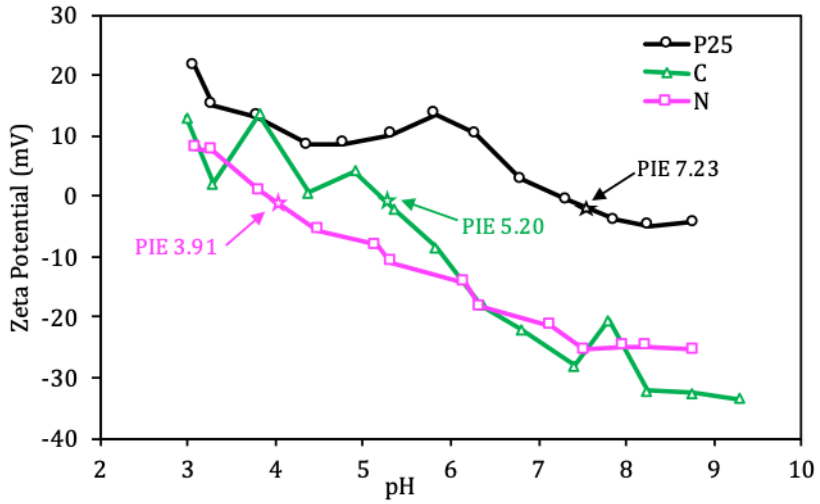

Figure 5: Zeta potential of the nano-TiO_2 powders.

Figure 6 presents the flowability of the mortars in terms of spread on table. For industrialized mortars (Figure 6 (a)), the REF industrialized series obtained 21.6 cm of spread, and it is possible to verify that the nano-TiO_2 addition reduced the flowability of the mortars. For industrialized mortars with C and P25 nano-TiO_2, an effective reduction was verified only with 10% of nanotitania. For C type, this may be justified by the coarse particles, as evidenced in Figure 3. When N-type were added, there was a great reduction in the spread on table at 5% of nano-TiO_2 addition. However, after 7% nano-TiO_2, the spread increased for similar values obtained for other nano-TiO_2 types. This may be attributed to the agglomeration of the nanopowder added in high amounts to cementitious mortars. The agglomeration reduces the surface and results in less water absorption that reflects in higher spread values, in comparison with the non-industrialized 7% sample. There is also a great effect of the content and size of air bubbles and microbubbles on the spreading (and, in general, on the rheological behavior) of the cementitious mortars promoted by the air-entraining admixture.

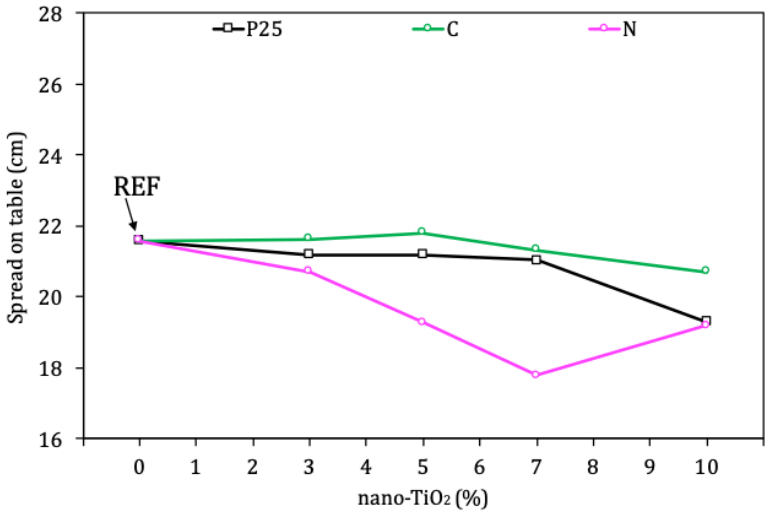

(a)

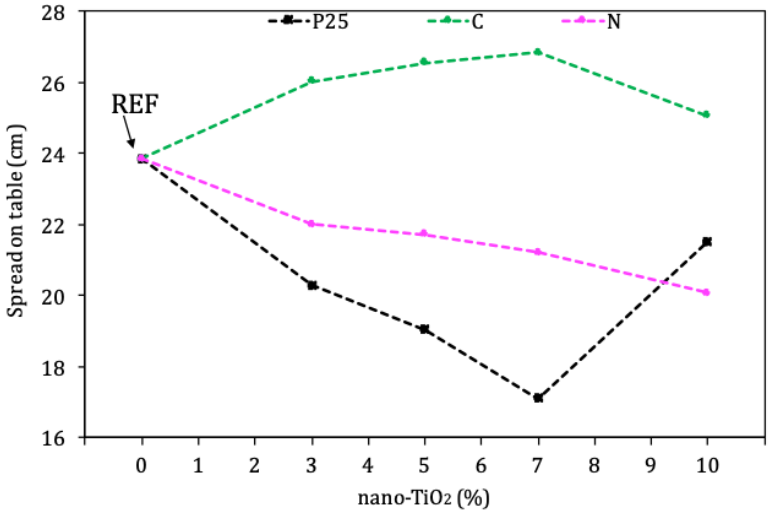

(b)

Figure 6: Flowability of the nano-TiO_2 samples: (a) Industrialized mortars; (b) Non-industrialized mortars.

For non-industrialized mortars (Figure 6 (b)), the flowability behavior was considerable different. The non-industrialized REF series resulted in 23.9 cm, which was higher than the reference value of industrialized mortars. This may be explained by the presence of superplasticizer admixture in the composition of the cementitious mortars. It is possible to note that for N nano-TiO_2 addition, the higher the

amount of the nanopowder, the lower the spread. As expected, this is due the higher surface area available to water/admixture adsorption. The P25 addition presented the same trend. However, the addition of 10% nano-TiO_2 lead to an increase in the spread on table, indicating that this amount of nanotitania may result in particle agglomeration, reducing the potential of the powder surface for interaction with the water/admixture of the mixture, which reflects in higher spread on table values. On the other hand, the C nano-TiO_2 addition resulted in an increase of spread value until 7% of nanopowder. This is justified by the coarse particles in comparison with other nanoparticles used. Finally, with 10% of nanotitania addition, the spread reduced, which may be justified also by the high amount of particles. Even though, they are coarse, they present high specific areas that may interact with me mixture and reduce the water or admixture in the material.

In Figure 7, the sand height (SH) shows, indirectly, the roughness of the mortars surface. In the industrialized mortars (Figure 7 (a)), the REF sample obtained a SH of $520 \cdot 10^{-6}$ m and for C and N nano-TiO_2 added mortars, the higher the nanoparticles in the mixture, the lower the sand height, indicating a smooth surface as the higher the nanoparticles amount. However, for samples with P25, it was verified a low roughness increase up to 5% nanoparticles addition, a high increase for the 7% sample, and a substantial decrease for the 10% sample. This may be related to variation of samples finishing, which, in this case (coating mortar), is extremely dependent on the operator. As can be seen, it is possible to identify a tendency from 0 to 10% of nanoparticles addition, which is similar to the observed for N and C. This behavior suggests that the nanopowder may fill the porosity or improve the macrotexture of the mortar, lowering the roughness of the mortars surface.

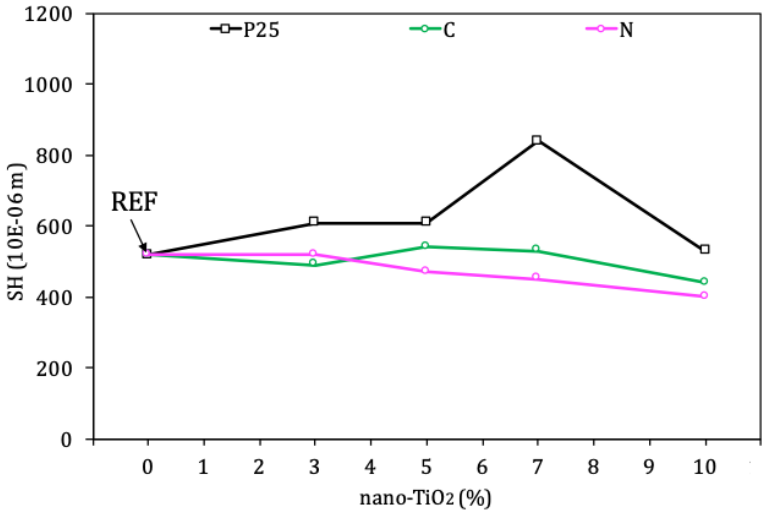

(a)

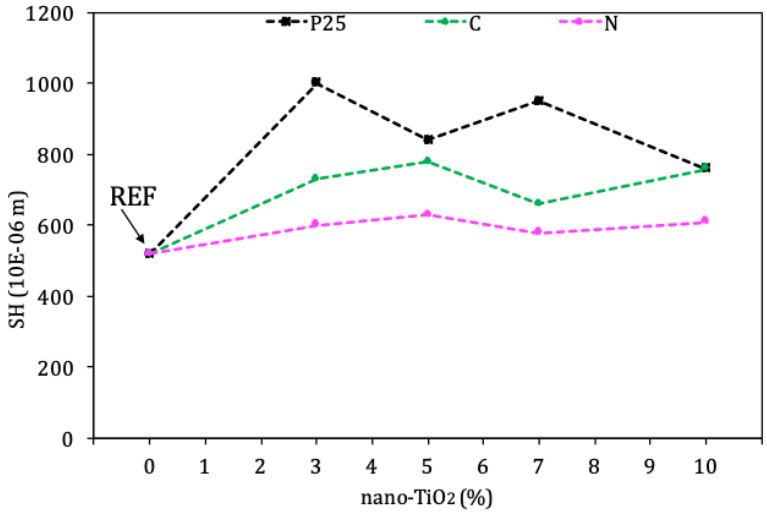

(b)

Figure 7: Sand height for: (a) Industrialized mortars; (b) Non-industrialized mortars.

On the other hand, for non-industrialized mortars (Figure 7 (b)), in general, the higher the nano-TiO_2

amount, the higher the SH in the mortars, indicating a roughness increased of the mortars surface. The N and C series presented a similar behavior, with C series showing higher values than N series. However, the series with P25 presented a high increase in SH from 0 to 3% of nanoparticles, then a SH decrease until 10% of nanopowder addition. A justification that may explain the higher roughness observed in non-industrialized mortars is the composition of the mortars, that presents the ratio cement: aggregates 1:6 in comparison to industrialized mortars that present ratio 1:4. This configuration results in a rougher surface due the higher aggregate content. This is also reinforced once as the higher cement, the higher the water content (for a constant water/binder ratio), that promotes a better fluidity/lubrication of the aggregates of the mortar and may result in a better surface finishing.

Figure 8 presents the flexural strength of the mortars. For industrialized mortars (Figure 8 (a)), the reference series presented a flexural strength of 1.10 MPa. Series with P25 presented a progressive evolution of flexural strength as the higher the nanoparticles amount. However, the series with N and C nanotitania presented a high increase in the strength already with 3%. The higher the nanoparticles presence, the lower was the mechanical behavior. This behavior may be related to zeta potential of the nanoparticles (Figure 5), which for P25 showed a higher tendency to agglomerate in neutral and basic environmental than the other nanoparticles used. This reflected that there was a low efficiency of P25 nano-TiO_2 in improving the mechanical properties in comparison with other nanopowders. For N and C types, when a small amount of nanoparticles are present, the basic environment is enough to promote an effective dispersion of the particles, resulting in a homogeneous filling/interaction with cement/binder particles in the moment of hydration, reflecting in the higher values of flexural strengths even with 3% of nanoparticles. Therefore, the lower mechanical performance with higher amounts of nanotitania may be due to the saturation of the mixture. For these types of nanopowders, 3% of nanoparticles is already efficient and no more addition is necessary.

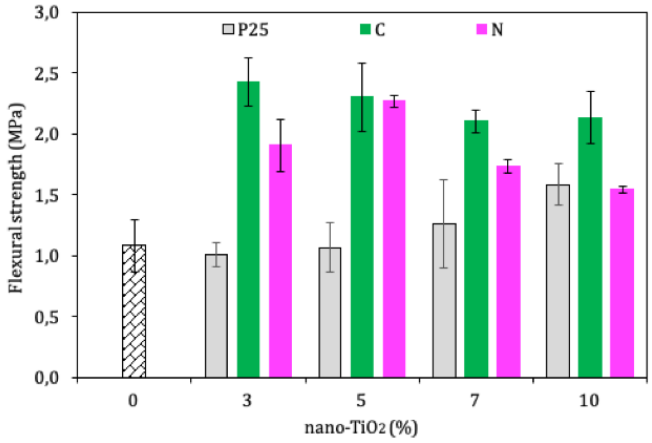

(a)

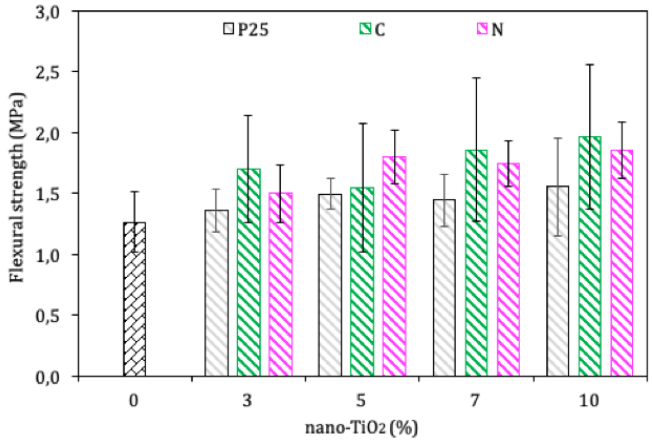

(b)

Figure 8: Flexural strength: (a) Industrialized mortars; (b) Non-industrialized mortars.

For non-industrialized mortars (Figure 8 (b)), the reference series presented a flexural strength of 1.27

MPa, that is 27% higher than industrialized reference series and it is attributed to the lower water/binder ratio. In the non-industrialized series with nano-TiO_2, the higher the nanopowder addition, the higher the improvement in the mechanical performance. It is verified a sensible enhancement from 3 to 10% of nano-TiO_2 powders; however, the standard deviation of the samples clearly overlaps with the reference sample, which is expected for the flexural test, mainly for brittle materials, as cementitious mortars. Nevertheless, it is possible to note that there was a progressive improvement of the mechanical strength, which may be attributed to the filling effect, resulting in a denser material. Alternatively, the seeding effect might have promoted ionized surface for cement products precipitation, improving the cement hydration index, due to the lower water/binder ratio.

Figure 9 presents the microstructural fracture surface of the reference mortars and mortars with 3% of nano-TiO_2 and the respective semi-quantitative chemical analysis by EDS. For reference mortars (Figure 9 (a) and (b)), it is possible to note that the surface of industrialized mortar is smoother than that of non-industrialized mortars, due to the higher water/binder ratio. However, in both surfaces it is verified a great degree of macroporosity, which is typical due to the high water/binder ratio of both types of cementitious mortars. In the chemical analysis, the same trend was verified with calcium and silicon (from C-S-H) as main compounds present in the material.

For samples with nano-TiO_2 (Figure 9 (c), (d), (e), (f), (g), (h)), cracks were identified in the fracture surface, which are more tortuous in comparison with the reference series. It is possible to note that in some regions of the fracture surface, parts of the aggregates are exposed, due to the lower mechanical properties in this part of the composite. This is expected in the cementitious matrix region, also known as interfacial transition zone (ITZ). When the cementitious matrix is tensioned, the cracks tend to nucleate around this area, which is normally composed by a higher water/binder ratio (due the aggregates water absorption), in comparison with the bulk matrix. Then, the crack is more likely in this region but may deviate from ITZ and grow in bulk direction, as verified.

The chemical analysis for the mortars with nanoadditives are very similar. A Ti peak was identified, nevertheless, with only a small intensity, as expected, due the low amount of nano-TiO_2 present in the samples. Moreover, there is a great part of the nanoparticles that are in the bulk part of the material, considering a homogeneous dispersion.

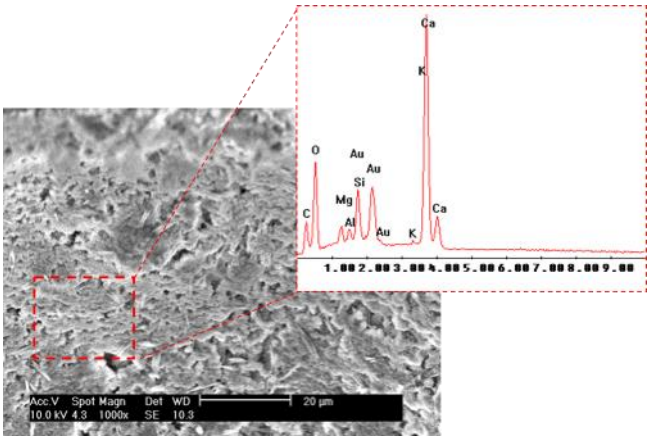

(a) REF_I.

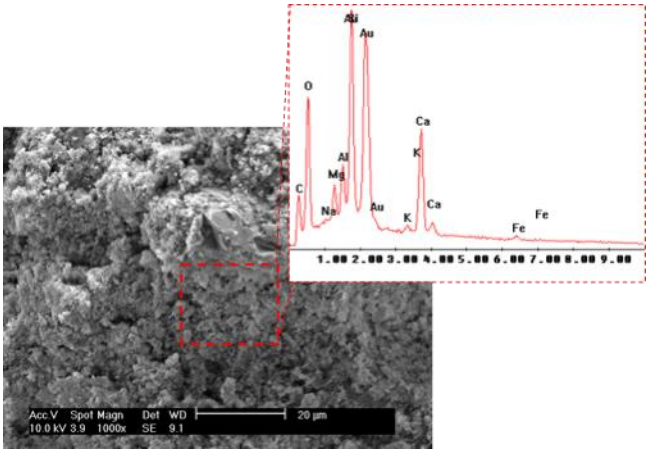

(b) REF_N.

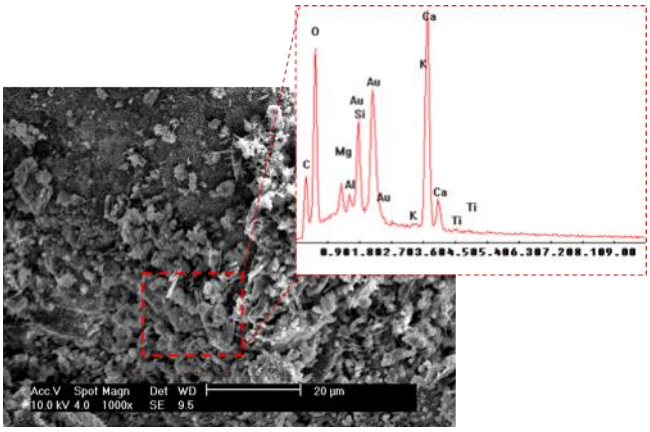

(c) I_3% with P25 nano-TiO_2.

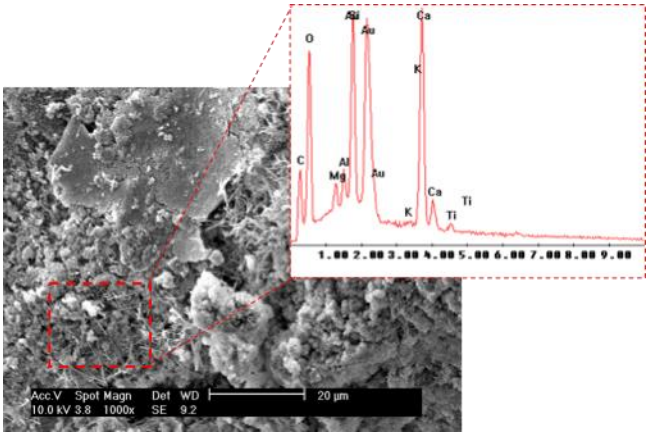

(d) N_3% with P25 nano-TiO_2.

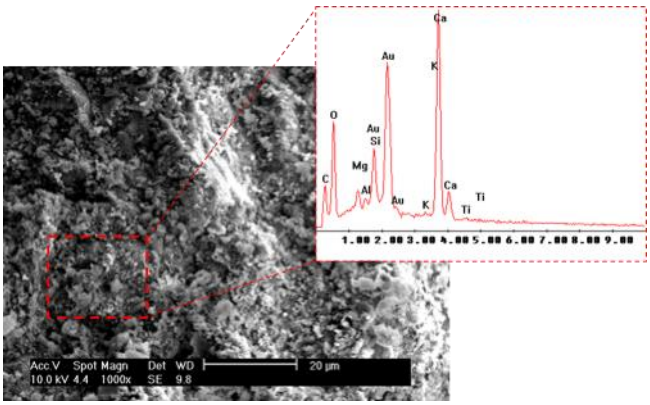

(e) I_3% with C nano-TiO_2.

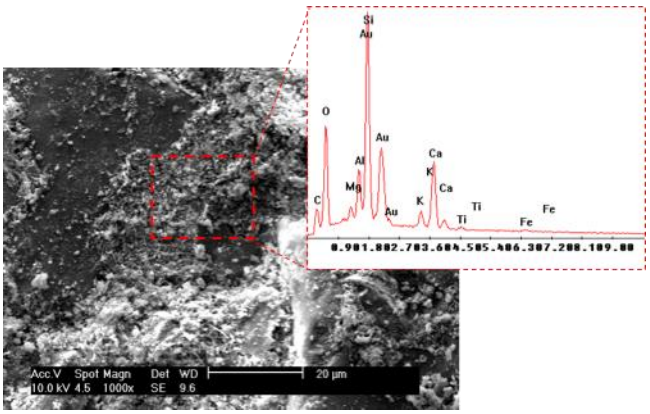

(f) N_3% with C nano-TiO_2.

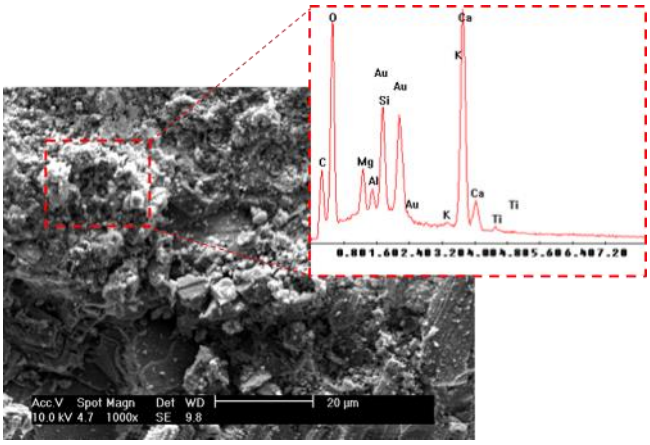

(g) I_3% with N nano-TiO_2.

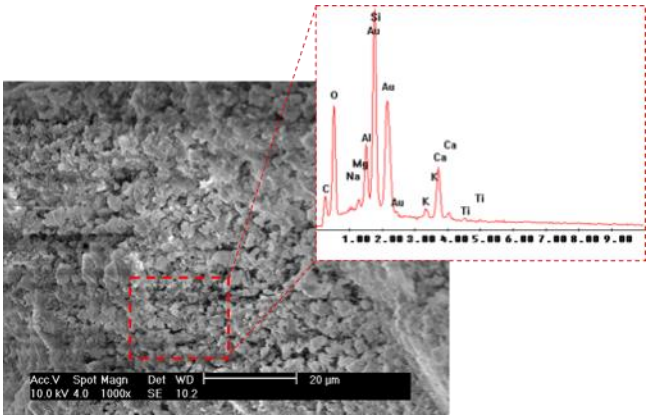

(h) N_3% with N nano-TiO_2.

Figure 9: Microstructure of the 3% nano-TiO_2-added mortars surface.

4. CONCLUSION

This work evaluated the feasibility of using nano-TiO_2 powders in cementitious mortars. Based on results obtained, the following conclusions may be drawn:

- The commercial nano-TiO_2 available presented different characteristics, as PSD, zeta potential, PIE, BET and microstructures. These differences are determinant in the fresh and hardened properties of the cementitious mortars;
- The type of the mortar also is a relevant item that has to be analyzed in the production process. In this work, different fresh and hardened properties were obtained with the mortars used, indicating that even similar composition of the mortars may not present similar trend in the properties in fresh and hardened state;
- The nano-TiO_2 addition influences the flowability of the mortars; in general, decreasing the spread on table, mainly due to the additional specific surface area that adsorbs part of the admixture and/or water;
- The macroporosity is also affected by nano-TiO_2 addition. In general, for industrialized mortars, the higher the nanopowder amount, the smoother the surface. For the non-industrialized mortars, the higher the nanopowder amount, the rougher the surface;
- For mechanical properties, in the non-industrialized mortars, a proportional trend was observed, as the higher the amount of the nanoparticles in the mortars, the higher the mechanical performance. For industrialized mortar, only samples with P25 presented a progressive trend. This suggests that the mortar proportion is also relevant in the final mechanical behavior of the material. 3% nano-TiO_2 seems to be enough for enhancement of flexural strength;
- The SEM surface analysis showed that the fracture is tortuous and tends to grow at the ITZ around the aggregate.

In addition, these results contribute to the choice of nano-TiO_2 or general nanopowders as material replacement in the construction industry. However, further studies are required such as evaluating durability and metal leaching.

5. ACKNOWLEDGMENT

The authors would like to thank to LINDEN-UFSC through NanoTec and LCME-UFSC laboratories for the support during the experimental program; to Cimentos Votorantim for the financial support of the research, in addition to Brazilian governmental research agencies, Coordination for the Improvement of Higher Education Personnel (CAPES) and National Council for Scientific and Technological Development (CNPq) for the financial support to laboratories.

6. REFERENCES

[1] JOCHEM, L.F.; APONTE, D.; BIZINOTTO, M.B.; *et al.,*"Effects of pre-wetting aggregate on the properties of mortars made with recycled concrete and lightweight aggregates", *Matéria (Rio Janeiro),* n. 24, 2019.

[2] ASSOCIAÇÃO BRASILEIRA DE NORMAS TÉCNICAS, NBR 13281 - Argamassa Para Assentamento e Revestimento de Paredes e Tetos - Requisitos, Rio de Janeiro, 2005.

[3] KORAYEM, A.H.; TOURANI, N.; ZAKERTABRIZI, M.; *et al.,* "A review of dispersion of nanoparticles in cementitious matrices: Nanoparticle geometry perspective", *Construction and Building Materials*, n.153, pp.346-357, 2017.

[4] SINGH, L.P.; KARADE, S.R.; BHATTACHARYYA, S.K.; *et al.,* "Beneficial role of nanosilica in cement based materials - A review", *Construction and Building Materials,* n.47, pp.1069-1077, 2013.

[5] CASAGRANDE, C.A.; CAVALARO, S.H.P.; REPETTE, W.L. "Ultra-high performance fibre-reinforced cementitious composite with steel microfibres functionalized with silane", *Construction and Building Materials*, n.178, pp.495-506, 2018.

[6] SENFF, L.; LABRINCHA, J.A.; FERREIRA, V.M.; *et al.,* "Effect of nano-silica on rheology and fresh properties of cement pastes and mortars", *Construction and Building Materials,* n.23, pp.2487-2491, 2009.

[7] SENFF, L.; HOTZA, D.; LUCAS, S.; *et al.,* "Effect of nano-SiO2 and nano-TiO2 addition on the rheological behavior and the hardened properties of cement mortars", *Materials Science and Engineering. Part A*, n.532, pp.354-361, 2012.

[8] SENFF, L.; BARBETTA, P. A.; REPETTE, W.L.; *et al.*, "Mortar composition defined according to rheometer and flow table tests using factorial designed experiments", *Construction and Building Materials*, n.23, pp.3107-3111, 2009.

[9] OERTEL, T.; HELBIG, U.; HUTTER, F.; *et al.*, "Influence of amorphous silica on the hydration in ultra-high performance concrete", *Cement and Concrete Research*, n.58, pp.121-130, 2014.

[10] SINGH, L.P.; BHATTACHARYYA, S.K.; SHAH, S.P.; *et al.*, "Studies on early stage hydration of tricalcium silicate incorporating silica nanoparticles: Part II", *Construction and Building Materials*, n.102, pp.943-949, 2016.

[11] SCRIVENER, K.L.; KIRKPATRICK, R.J. "Innovation in use and research on cementitious material", *Cement and Concrete Research*, n.38, pp.128–136, 2008.

[12] LAND, G.; STEPHAN, D. "Controlling cement hydration with nanoparticles", Cement and Concrete Composites, n.57, pp.64-67, 2015.

[13] SENFF, L.; TOBALDI, D.D.M.; LUCAS, S.; *et al.*, "Formulation of mortars with nano-SiO2 and nano-TiO2 for degradation of pollutants in buildings", *Composites Part B: Engineering*, n.44, pp.40-47, 2013.

[14] CASAGRANDE, C.A.; REPETTE, W.L.; GLEIZE, P.J.P.; *et al.*, "Environmental Effects on the Photocatalytic Efficiency (NOx Reduction) of Nanotitania in Portland Cement Mortar", In: K. Sobolev, S.P. Shah (eds.), "*Nanotechnology in Construction*", Springer International Publishing, Cham, pp. 347-353, 2015.

[15] CASAGRANDE, C.A. "*Desenvolvimento de argamassas com incorporação de nanopartículas de dióxido de titânio*", dissertação de mestrado, Universidade Federal de Santa Catarina – UFSC, Florianópolis, SC, 2012.

[16] CÁRDENAS, C.; TOBÓN, J.I.; GARCÍA, C.; *et al.*, "Functionalized building materials: Photocatalytic abatement of NOx by cement pastes blended with TiO2 nanoparticles", *Construction and Building Materials*, n.36, pp.820-825, 2012.

[17] FUJISHIMA, A.; ZHANG, X.; TRYK, D. "TiO2 photocatalysis and related surface phenomena", *Surface Science Reports*, n.63, pp.515-582, 2008.

[18] ASSOCIAÇÃO BRASILEIRA DE NORMAS TÉCNICAS, NBR 13276 - Argamassa para assentamento e revestimento de paredes e tetos - Preparo da mistura e determinação do índice de consistência, Rio de Janeiro, 2016.

[19] ASSOCIAÇÃO BRASILEIRA DE NORMAS TÉCNICAS, NBR 13279 - Argamassa para assentamento e revestimento de paredes e tetos - Determinação da resistência à tração na flexão e à compressão, Rio de Janeiro, 2005.

[20] AMERICAN SOCIETY OF TESTING MATERIALS, ASTM E965 - Standard Test Method for Measuring Pavement Macrotexture Depth Using a Volumetric Technique, West Conshohocken, 2015.

[21] OHTANI, B.; PRIETO-MAHANEY, O.O.; LI, D.; *et al.*, "What is Degussa (Evonik) P25? Crystalline composition analysis, reconstruction from isolated pure particles and photocatalytic activity test", *Journal of Photochemistry and Photobiology A: Chemistry*, n.216, pp.179-182, 2010.

[22] SCHNEIDER, J.; MATSUOKA, M.; TAKEUCHI, M.; *et al.*, "Understanding TiO2 Photocatalysis: Mechanisms and Materials", *Chemical Reviews*, n.114, pp.9919-9986, 2014.

[23] THIRUVENKATACHARI, R.; VIGNESWARAN, S.; MOON, I.S. "A review on UV/TiO2 photocatalytic oxidation process - Review", *Korean Journal of Chemical Engineering*, n.25, pp.64-72, 2008.

[24] DE MELO, J.V.S.; TRICHÊS, G. "Evaluation of the influence of environmental conditions on the efficiency of photocatalytic coatings in the degradation of nitrogen oxides (NOx)", *Building and Environment*, n.49, pp.117-123, 2012.

[25] RUOT, B.; PLASSAIS, A.; OLIVE, F.; *et al.*, "TiO2-containing cement pastes and mortars: Measurements of the photocatalytic efficiency using a rhodamine B-based colorimetric test", *Solar Energy*, n.83, pp.1794-1801, 2009.

[26] LEINEKUGEL-LE-COCQ-ERRIEN, A.Y.; DENIARD, P.; JOBIC, S.; *et al.*, "Structural characterization of the hollandite host lattice for the confinement of radioactive cesium: Quantification of the amorphous phase taking into account the incommensurate modulated character of the crystallized part", *Journal of Solid State Chemistry*, n.180, pp.322-330, 2007.

[27] TOBALDI, D.M.; TUCCI, A.; ŠKAPIN, A.S.; *et al.*, "Effects of SiO2 addition on TiO2 crystal structure and photocatalytic activity", *Journal of the European Ceramic Society*, n.30, pp.2481-2490, 2010.

ORCID

Cézar Augusto Casagrande https://orcid.org/0000-0002-4293-6574
Lidiane Fernanda Jochem https://orcid.org/0000-0001-6679-2897
Wellington Longuini Repette https://orcid.org/0000-0003-0697-2794
Dachamir Hotza https://orcid.org/0000-0002-7086-3085